Eur. Phys. J. B **26**, 23–28 (2002)
DOI: 10.1140/epjb/e20020061

THE EUROPEAN PHYSICAL JOURNAL B
EDP Sciences

Strain effect on transport properties of $SrRuO_3$ films grown by laser MBE

P. Orgiani[a], C. Aruta, G. Balestrino, S. Lavanga, P.G. Medaglia, and A. Tebano

INFM- Dipartimento Scienze e Tecnologie Fisiche ed Energetiche, Univeristà di Roma "Tor Vergata", Via del Politecnico 1, 00133 Roma, Italy

Received 16 July 2001 and Received in final form 22 October 2001

Abstract. Transport properties of $SrRuO_3$ thin films were studied as a function of the epitaxial strain. $SrRuO_3$ films were grown on (100) $SrTiO_3$ substrates by the Pulsed Laser Deposition technique equipped with Reflection High Energy Electrons Diffraction (RHEED). Samples thickness has been varied from a few unit cells to above 1000 Å while monitoring RHEED intensity oscillations. In thicker films epitaxial strain was found to be progressively relaxed. $SrRuO_3$ relaxed films (thickness $\gtrsim$ 1000 Å) show metallic behavior for the whole temperature range with a ferromagnetic ordering at about 150 K. For thinner films, ferromagnetic ordering occurs at progressively lower temperatures, until in films thinner than 400 Å it disappears. Films thinner than 80 Å show a semiconducting behavior at low temperatures. Our results provide direct evidence of the crucial role of the strain effect for conducting and magnetic properties of $SrRuO_3$.

PACS. 81.15.Fg Laser deposition – 75.70.Ak Magnetic properties of monolayers and thin films – 81.40.Jj Elasticity and anelasticity, stress-strain relations

The family of perovskite oxides displays a large variety of technologically important phenomena such as high temperature superconductivity, ferroelectricity, ferromagnetism, colossal magnetoresistance and metallic conductivity. The structural and chemical similarities of these materials make the growth of epitaxial heterostructures possible, thus opening new perspectives in the field of electronic, magnetic and optical devices. Because of its electrical transport and magnetic [1,2] properties $SrRuO_3$ represents a very interesting model material for the study of itinerant magnetism in oxide systems [3]. Moreover due to its structural compatibility with high temperature superconductors, such as $YBa_2Cu_3O_{7-\delta}$ [4], $SrRuO_3$ can be very promising for possible applications in the field of integrated spintronics [5].

The $SrRuO_3$ crystal structure was found to be orthorhombic with lattice constants $a^0 = 5.56$ Å, $b^0 = 5.53$ Å and $c^0 = 7.84$ Å. It has a subunit cell that is a pseudocubic perovskite with lattice constants $a^p \cong b^p \cong c^p = 3.93$ Å for bulk material [1] and slightly larger, *i.e.* 3.94 Å, for epitaxial films [6]. For the sake of simplicity in this paper, the Miller' indices of $SrRuO_3$ will be referred to the perovskite cell (indicated by the superscript p). $SrRuO_3$ shows a ferromagnetic transition at a Curie temperature of $\sim 150 \div 160$ K [2]. Even if the origin of the ferromagnetic ordering is not completely cleared up [3,7,8], several works have given preliminary evidence of a strong correlation between transport, magnetic and structural properties of $SrRuO_3$ [9–14]. In the distorted $SrRuO_3$ perovskite, the RuO_2 planes are *corrugated*, in the sense that the O atoms are slightly displaced out of the planes of the Ru atoms. A microstructural parameter characterizing such distortion is the angle between the Ru-O bond and the Ru-*plane* (*buckling angle*). Studies on ruthenate compounds suggest that the Ru-O-Ru structural arrangement is crucial for the magnetic properties of this material [15–18]. A mechanism influencing the Ru-O-Ru arrangement in $SrRuO_3$ films is the epitaxial strain induced by the substrates. In the case of the $SrTiO_3$ substrate, due to the relatively small mismatch between film and substrate lattice parameters (less than 1%), it is possible to obtain coherently strained thin $SrRuO_3$ films. However above a certain critical thickness, the epitaxial strain is progressively relaxed until, for thick films, the $SrRuO_3$ lattice parameter approaches the bulk value. The buckling angle for $SrRuO_3$ relaxed films was found to be about 6.6° [19]. The *in-plane* strain (ε_{ab}) is defined as the difference between the bulk and the strained film lattice parameters, normalized to the bulk value. Because of the Poisson effect, the compression of the $SrRuO_3$ cell in the Ru plane ($\varepsilon_{ab} > 0$) produces an increase in the lattice parameter along the $c^p - axis$ direction. Reasonably both the

[a] e-mail: pasquale.orgiani@na.infn.it

interatomic distance between the alkaline earths and the oxygen ions in the Ru planes and the distance between Ru and the octahedrally coordinated oxygens remain almost constant. This feature results in an increase of the Ru-O buckling angle.

The aim of this work is the study of the influence of the epitaxial strain on the electrical and magnetic properties of $SrRuO_3$ films. Nevertheless, the study of the relationship between structural and transport properties strongly depends on the capability to obtain high quality heteroepitaxial films. In the last few years, several research groups have been able to use pulsed laser deposition (PLD) equipped with *in situ* Reflection High Energy Electron Diffraction (RHEED) analysis, *i.e.* laser molecular-beam epitaxy (Laser MBE) to obtain the 2-dimensional (2D) growth of artificial materials. Laser MBE guarantees the required control on the $SrRuO_3$ film growth and on the crystallographic quality of the substrate-film interface. Different strain values were obtained varying the $SrRuO_3$ film thickness from ultrathin (few unit cells) to thick ($\gtrsim$ 1000 Å) layers.

$SrRuO_3$ films were deposited on (100) $SrTiO_3$ single crystal substrates (with lattice parameters $a = 3.904$ Å) by Pulsed Laser Deposition (PLD) technique using a KrF excimer pulsed laser source ($\lambda = 248$ nm), with a typical energy density of about 3 J/cm^2. Nominally all substrates had zero miscut. Following the procedure of Kawasaki *et al.*, the substrates were etched prior to deposition in buffered HF solution to provide a smooth TiO_2-terminated growth template [20]. Films were grown starting from a $SrRuO_3$ stoichiometric target. The growth temperature ranged from 450 °C to 570 °C. Recent powder X-ray diffraction experiments show a transition from an orthorhombic phase, at room temperature, to a tetragonal phase at higher temperature [21,22]. In order to analyze the effect of such a structural transition on the film strain, several samples were grown varying the deposition temperature. For our growth condition, we do not detect any sizeable effect of growth temperatures on the film strain. $SrRuO_3$ films were grown at different oxygen pressures (from 10^{-4} to 10^0 mbar). The magnetoresistance and electrical resistivity properties resulted to be independent from oxygen pressure. This feature made possible the $SrRuO_3$ films growth by Laser MBE (namely at an oxygen pressure $\lesssim 10^{-4}$ mbar) using the RHEED control. The deposition process was monitored by *in situ* RHEED analysis. The direct calibration of the deposition rate through the intensity oscillation of the specular diffraction spot in the RHEED pattern guaranteed the precise control of the film thickness. For all samples, structural characterization was carried out by X-ray diffraction using Cu K_α radiation. Resistance measurements were performed by a standard four-probe DC technique.

RHEED oscillations of a typical $SrRuO_3$ film, detected at the first deposition stage, are shown in Figure 1a. In accordance with the well accepted interpretation, a complete oscillation in the intensity of the RHEED pattern corresponds to the growth of one unit cell. There is a sizeable difference between the first oscillation width and the following ones. As shown in a recent work, this difference is probably due to a change in the mobility of the adatoms, switching the surface termination layer from the substrate to the film [23]. Nevertheless starting from the second oscillation in the RHEED pattern, the number of the laser shots to complete one oscillation resulted to be constant. The possibility to monitor the deposition process by RHEED analysis, combined with the very low deposition rate (about 35÷40 laser shots per unit cell starting from the second oscillation), allows a precise control of the film thickness.Moreover, the RHEED pattern maintains a 2D nature for the whole deposition process. In Figure 1b the final 2D pattern is shown for a $SrRuO_3$ film about 1000 Å thick. $SrRuO_3$ epitaxial films were also grown on (100) $LaAlO_3$ and (110) $NdGaO_3$ substrates (with *in-plane* lattice parameter of 3.79 Å and 3.85 Å respectively). Due to the larger mismatch with the $SrRuO_3$ lattice parameter, the epitaxial strain is already relaxed in the first few layers [9]. As a consequence the growth on such substrates was not pure 2D and no oscillations in RHEED pattern were detected.

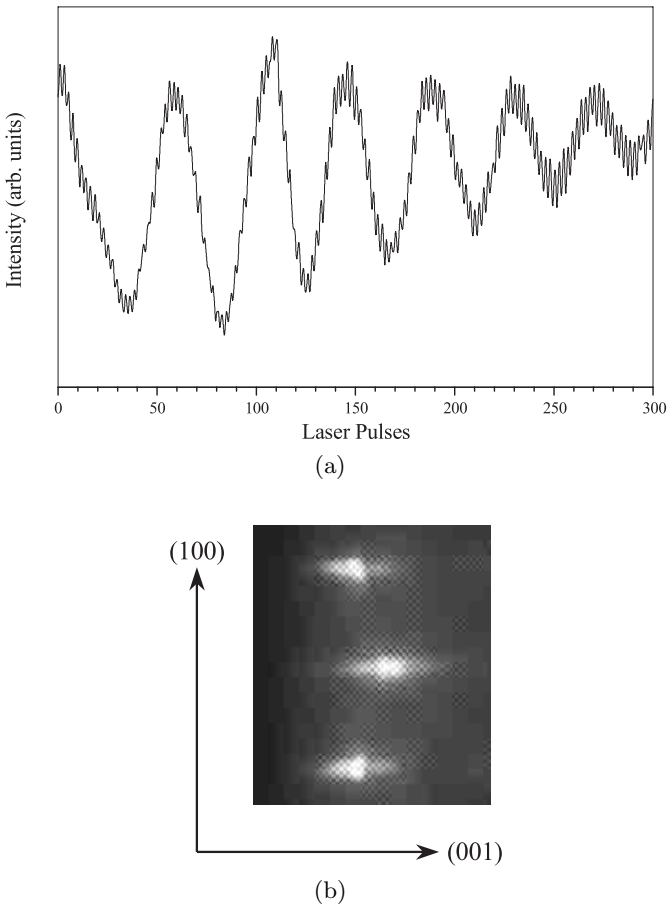

Fig. 1. (a) RHEED intensity oscillations of the specular spot during the $SrRuO_3$ film growth as a function of laser pulses. (b) Typical 2D final RHEED pattern of the $SrRuO_3$ surface.

Standard X-ray diffraction (XRD) characterization was performed for all samples. $\theta - 2\theta$ XRD diffraction

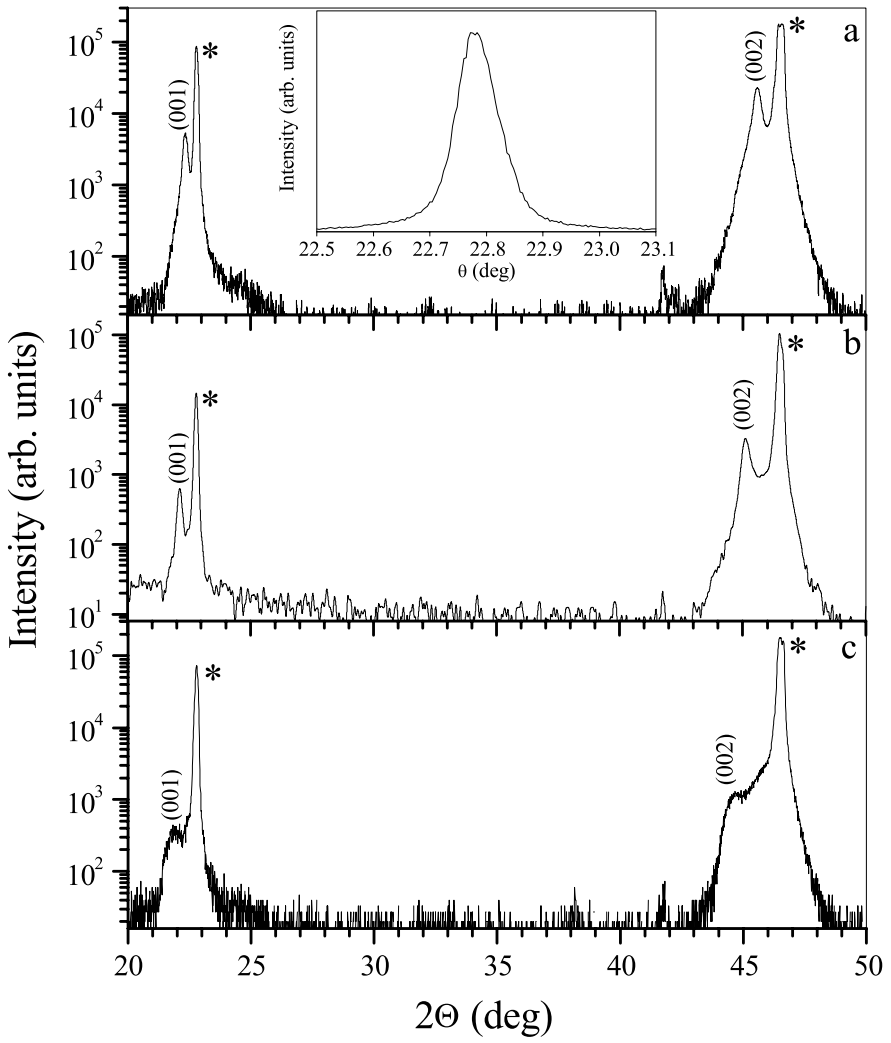

Fig. 2. $\theta - 2\theta$ XRD spectra of three $SrRuO_3$ films grown on (001) $SrTiO_3$ substrate (*); the film thickness are 1000 Å (a), 400 Å (b) and 80 Å (c) respectively. In the inset of Figure 2a typical XRD $\omega - scan$ of the $(002)^p$ $SrRuO_3$ reflection.

patterns show only the $(00l)^p$ peaks, indicating that films are $[001]^p$ oriented. A typical XRD spectrum of a $SrRuO_3$ thick film (1000 Å) is reported in Figure 2a. To check the crystalline quality of the films, rocking curve measurements were also performed (inset Fig. 2a). For thick films typical full width at half maximum (FWHM) of the rocking curve for the $(002)^p$ reflection is about 0.1°. The c^p lattice parameter of films having thickness larger than 1000 Å results to be 3.96 Å (as reported in literature, the c^p lattice parameter of epitaxial films results to be slightly larger than the 3.93 Å bulk value). On the contrary, thinner films are heavily strained. As a consequence of the *in-plane* compressive epitaxial strain, a sizable increase of the c^p lattice parameter occurs. $\theta - 2\theta$ XRD spectra for three $SrRuO_3$ samples with different thickness (1000 Å, 400 Å and 80 Å respectively) are reported in Figure 2. Thinner films are more and more strained and as a consequence a shift of the $(00l)^p$ $SrRuO_3$ diffraction peaks toward lower angles is detected. The c^p lattice parameter values, calculated for 1000 Å, 400 Å and 80 Å thick films, result to be 3.96 Å, 4.01 Å and 4.06 Å (±0.01) respectively. The in-plane a^p lattice parameter was also measured. Using asymmetric $(303)^p$ reflection, a^p was found to be 3.93 Å and 3.91 Å (±0.02) for 1000 Å and 400 Å thick films respectively. Moreover ϕ-scan mmeasurements (Fig. 3) show that the $SrRuO_3$ films grow with the *in-plane* a^p axis perfectly aligned with the $SrTiO_3$ substrate ones. The above values confirm that the relaxed film lattice parameters are slightly larger than bulk ones [22].

Electrical transport measurements were carried out by standard four-probe dc technique, with a bias pulsed and reversed current density of about 100 A/cm^2. The thickest sample (*a* in Fig. 4) shows electrical resistance and magnetoresistance properties very similar to those reported in literature for thick films. Namely, for films thicker than 1000 Å, the resistivity behaviour is metallic for the whole temperature range with a ferromagnetic transition at about 150 K. Values of the Residual

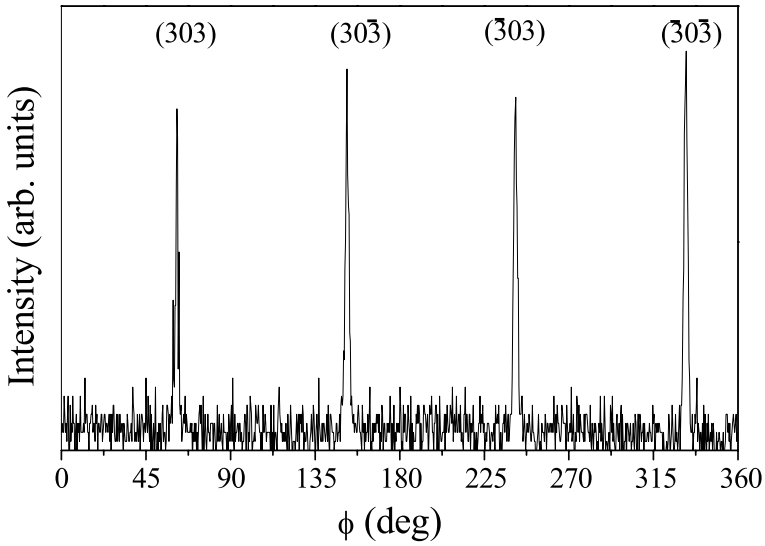

Fig. 3. $\phi - scan$ measurement of 400 Å thick $SrRuO_3$ films.

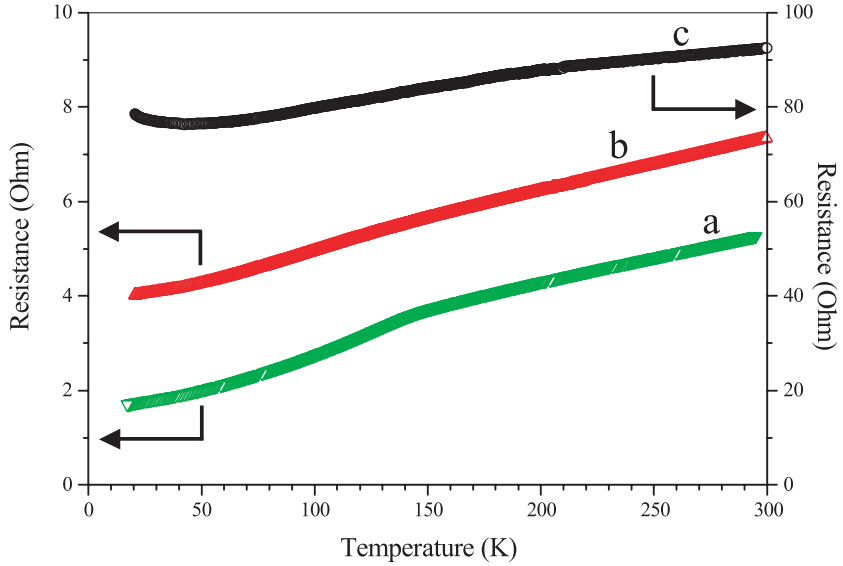

Fig. 4. Resistance *vs.* temperature for 1000 Å (*a*), 400 Å (*b*) and 80 Å (*c*) thick $SrRuO_3$ films.

Resistance Ratio (RRR, defined as the ratio between the resistance measured at 300 K and the value calculated from a linear extrapolation to 0 K) are similar to those reported in literature. But there is a striking difference between the RR-value (defined as the ratio between the measured values of the resistance at 300 K and at 0 K) in our best films and higher values reported elsewhere in literature [9]. Preliminary measurements on $SrRuO_3$ films grown on (0001) Al_2O_3 and (111) Si substrates show higher RR-values compared to those grown on (100) $SrTiO_3$ substrates (unpublished). These data seems to confirm that the origin of such RR-values is not related to crystallographic quality of the samples. Furthermore derivative analysis confirms the T^2 behaviour at low temperature (Fig. 5a) [1]. Magnetoresistance measurements were performed with the applied magnetic field parallel to the electric current, namely in the Longitudinal Magneto Resistance configuration (LMR). A zero-field cooled resistance measurement and a magneto-resistance measurement in a field of 1.2 T were carried out as a function of the temperature. Measurements in a magnetic field were performed cooling the sample to 20 K in zero-field and then applying the external magnetic field. The difference between *zero-field* resistance and *in-field* resistance measurements in the vicinity of the Curie temperature is reported in Figure 5b. As expected, in the paramagnetic state ($T > T_C$) no difference between the two values is detected. In the ferromagnetic state ($T < T_C$), the external magnetic field increases the energy needed to flip a spin (where a conduction electron scatters, exchanging spin,

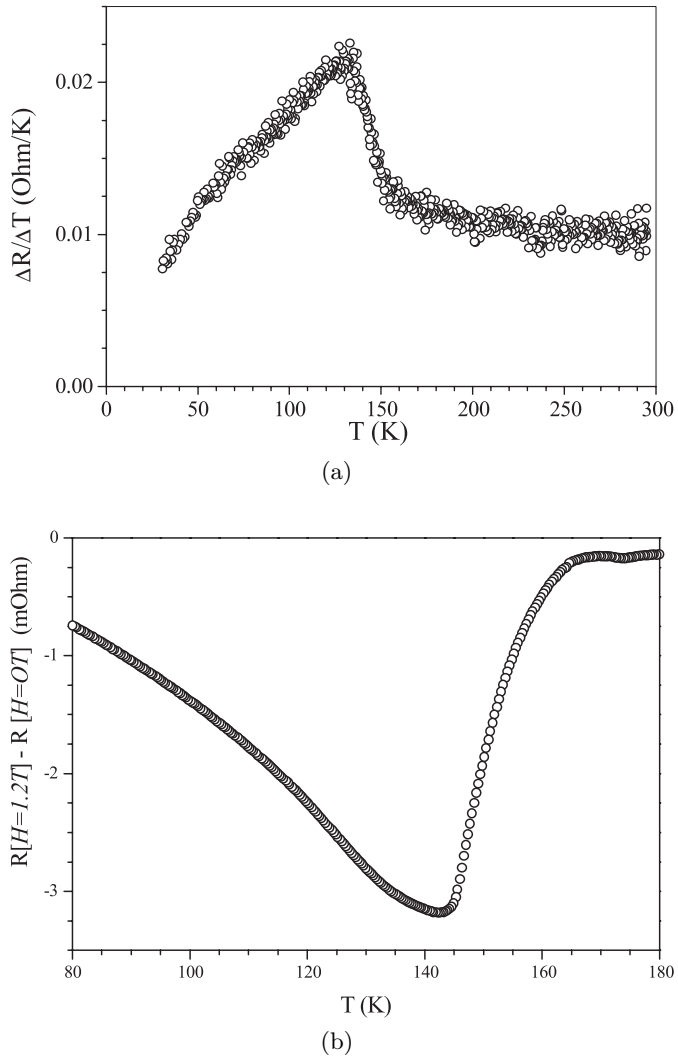

Fig. 5. (a) 1000 Å thick $SrRuO_3$ film resistance derivative *vs.* temperature. (b) difference between zero-field resistance and in-field resistance measurements as a function of temperature.

with a magnetic moment or spin excitation) and thus decreases the amplitude for the "spin-flip" scattering. As the external magnetic field increases the resistivity decreases. Decreasing the thickness, the ferromagnetic transition takes place at lower and lower temperatures. The ferromagnetic ordering disappears for a thickness smaller than few hundreds of Å. In particular the resistance of a 400 Å thick $SrRuO_3$ film is reported in Figure 4 (curve *b*). Even if the behaviour is metallic in the whole temperature range, no ferromagnetic transition occurs. A further decrease in the sample thickness, results in a metallic behaviour at relatively high temperatures and a semiconducting behaviour at low temperatures appears. In Figure 4 (curve *c*), the behaviour of resistance *versus* temperature is reported for a 80 Å thick $SrRuO_3$ film. A localization transition seems to take place at about $T \sim 30$ K.

All the data presented in this paper support the existing theories about the magnetic and conducting properties of $SrRuO_3$. As reported elsewhere [1,16], the feature that $SrRuO_3$ is both a good metal and a ferromagnetic material suggests that ferromagnetic ordering is due to Ru^{4d} band electrons. The width of the Ru^{4d} conduction band strongly depends on the superimposition of the oxygen O^{2p_σ} and O^{2p_π} orbitals and Ru^{4d} orbitals. In a relaxed structure (where the buckling angle has a minimum value) this superposition is maximized. As a consequence the conduction band width also has a maximum value and seems to be connected with the onset of the ferromagnetic ordering. Decreasing the film thickness, the strain contemporary induces an increase along the c^p-axis direction and a compression in the a^pb^p-*plane*. This feature results in an increase of the Ru-O buckling angle which, in turn, reduces the superposition of the ruthenium and the oxygen orbitals, decreasing the conduction band width. A semiconducting behaviour arises when the conduction band width becomes smaller than the localization energy.

In conclusion, the transport properties of $SrRuO_3$ films were studied as a function of strain effect. Epitaxial strain in the $SrRuO_3$ films was varied changing sample thickness from a few unit cells to hundreds of unit cells (∼1000 Å). Due to its small mismatch with the $SrTiO_3$ lattice parameter, $SrRuO_3$ epitaxial films were grown. All depositions processes were monitored by *in situ* RHEED pattern oscillations analysis. All samples exhibit very high crystallographic quality showing a pure 2D growth mechanism. Moreover, the RHEED pattern oscillations guaranteed a very precise control on the samples thickness. As expected the conducting and magnetic properties of $SrRuO_3$ films are strongly dependent on the epitaxial strain.

Relaxed films show metallic behaviour in the whole temperature range and a ferromagnetic ordering at about 150 K. As the thickness decreases (and consequently the strain increases), magnetic ordering does not occur even for films which are still metallic in the whole temperature range. Thin $SrRuO_3$ films (only a few unit cells thick) loose their metallic behaviour at low temperature showing a *semiconducting* behaviour below 30 K. The strong relationship between transport properties and magnetic properties confirms the itinerant nature of ferromagnetism in $SrRuO_3$ films.

References

1. G.S. Gausepohl, M. Lee, K. Char, R.A. Rao, C.B. Eom, Phys. Rev. B **52**, 3459 (1995).
2. P.B. Allen, H. Berger, O. Chauvet, L. Forro, T. Jarlborg, A. Junod, B. Revaz, G. Santi, Phys. Rev. B **53**, 4393 (1996).
3. L. Klein, J.S. Dodge, C.H. Ahn, G.J. Snyder, T.H. Geballe, M.R. Beasley, A. Kapitulnik, Phys. Rev. Lett. **72**, 2774 (1996).
4. X.D. Wu, S.R. Foltyn, R.C. Dye, Y. Coulter, R.E. Muenchausen, Appl. Phys. Lett. **62**, 2434 (1993).
5. S.A. Wolf, J. Supercond. **13**, 195 (2000).
6. J.P. Maria, D.G. Schlom, S. Troiler-McKinstry, M.E. Hawley, G.W. Brown, J. Appl. Phys. **83**, 4373 (1998).
7. R. Roussev, A.J. Lillis, Phys. Rev. Lett. **84**, 2279 (2000).

8. L. Klein, J.S. Dodge, C.H. Ahn, G.J. Snyder, T.H. Geballe, M.R. Beasley, A. Kapitulnik, Phys. Rev. Lett. **84**, 2280 (2000).
9. Q. Gan, R.A. Rao, C.B. Eom, J.L. Garrett, M. Lee, Appl. Phys. Lett. **72** , 978 (1998).
10. X.Q. Pan, J.C. Jiang, W. Tian, Q. Gan, R.A. Rao, C.B. Eom, J. Appl. Phys. **86**, 4188 (1999).
11. J.C. Jiang, X.Q. Pan, C.L. Chen, Appl. Phys. Lett. **72**, 909 (1998).
12. J.C. Jiang, W. Tian, X.Q. Pan, Q. Gan, C.B. Eom, Appl. Phys. Lett. **72**, 2963 (1998).
13. D.B. Kacedon, R.A. Rao, C.B. Eom, Appl. Phys. Lett. **71**, 1724 (1997).
14. Q. Gan, R.A. Rao, C.B. Eom, Appl. Phys. Lett. **70**, 1962 (1997).
15. G. Cao, S. McCall, M. Shepard, J.E. Crow, R.P. Guertin, Phys. Rev. B **56**, 321 (1997).
16. J.J. Nuemeier, A.L. Cornelius, J.S. Schilling, Physica B **198**, 324 (1994).
17. A. Kanbayasi, J. Phys. Soc. Jpn **44**, 108 (1978).
18. K. Ueda, H. Saeki, H. Tabata, T. Kawai, Sol. State Commun. **116**, 221 (2000).
19. H. Kobayashi, M. Nagata, R. Kano, Y. Kawamoto, Mater. Res. Bull. 1271 (1994).
20. M. Kavasaky, K. Takahashi, T. Maeda, R. Tsuschia, M. Shinohara, O. Ishiyama, M. Yoshimoto, H. Koinuma, Science **266**, 1540 (1994).
21. B.J. Kennedy, B.A. Hunter, Phys. Rev. B **58**, 653 (1998).
22. J.P. Maria, H.L. McKinstry, S. Troiler-McKinstry, Appl. Phys. Lett. **76**, 3382 (2000).
23. J. Choi, C.B. Eom, G. Rijnders, H. Rogalla, D.H.A. Blank, Appl. Phys. Lett. **79**, 1447 (2001).